LIQUID CRYSTALS, 2004, VOL. 31, NO. 6, 859–869

Taylor & Francis
Taylor & Francis Group

Planar and tilted uniform alignment of liquid crystals by plasma-treated substrates

O. YAROSHCHUK, R. KRAVCHUK, A. DOBROVOLSKYY, L. QIU† and O. D. LAVRENTOVICH*†‡

Department of Crystals, Institute of Physics of NASU, pr. Nauki 46, 03028 Kiev, Ukraine
†Liquid Crystal Institute, Kent State University, Kent, OH 44242, USA
‡Chemical Physics Interdisciplinary Program, Kent State University, Kent, OH 44242, USA

(*Received 6 February 2004; accepted 16 February 2004*)

We describe a new aligning technique that yields uniform planar or tilted orientation of a nematic liquid crystal at different organic and inorganic substrates. The method is based on the oblique irradiation of an aligning substrate with a partially collimated flux of accelerated plasma. The sheet-like plasma flux is produced by an anode layer thruster with a race track geometry of the discharge channel. For liquid crystals with a positive dielectric anisotropy the technique produces two modes of uniform alignment: (1) with the easy axis in the incident plane of the plasma beam; (2) with the easy axis perpendicular to the plane of incidence. Mode 1 transforms into mode 2 as the irradiation dose increases. In mode 1, the pretilt angle can be controlled by changing the parameters of irradiation such as incidence angle, current density and particle energy. In mode 2, the pretilt angle is zero (planar alignment). The azimuthal anchoring coefficient is relatively weak ($W_a \sim 10^{-6}\,\mathrm{J\,m^{-2}}$) for the first type of alignment and strong ($W_a \geqslant 10^{-4}\,\mathrm{J\,m^{-2}}$, comparable to rubbed polymer substrates) for the second type. The two-mode alignment feature can be used to control alignment properties and to create alignment patterns. The method is free from the usual shortcomings of the traditional rubbing technique. We discuss possible mechanisms of the two-mode alignment and show that plasma-induced modifications of the substrate topography might be an important factor in liquid crystal alignment.

1. Introduction

Liquid crystal (LC) cells used in displays and other applications are usually uniformly aligned. There are three basic types of LC alignment: (1) planar alignment with the LC director **n** parallel to one axis in the plane of substrate; (2) homeotropic alignment with **n** perpendicular to the substrate; (3) tilted LC alignment, the angle θ between the substrate and the director ('pretilt angle') being different from 0° and 90°. Many applications require tilted alignment with a small pretilt angle ($\theta < 10^\circ$).

A uniform alignment of LCs is usually achieved by an appropriate treatment of the bounding substrates. The prevailing technique for planar/tilted alignment is unidirectional rubbing of thin polymer films deposited onto the substrates. However, this method often causes surface deterioration, and the generation of electrostatic charges and dust on the aligning surfaces. Moreover, the rubbing technique is often hard to apply in situations where a non-trivial alignment pattern is needed, as, for example, in the so-called multidomain alignment.

Recent years have seen an increased interest in non-mechanical alignment techniques such as the photo-alignment method [1,2], in which light irradiation causes surface anisotropy of the bounding plates. The method is relatively simple and yields highly uniform planar or tilted alignment. However, the corresponding strength of alignment, quantified by the so-called anchoring energy coefficient, is relatively low; besides, some photoaligned substrates have poor photo and thermal stability. This appears to be caused by the relatively weak changes that a UV/visible beam can inflict upon the treated substrate. To strengthen the aligning action, a deep UV treatment has been suggested [3].

Another approach to non-mechanical planar or tilted planar alignment is a treatment with oblique particle beams [4–11]. The particles might be ions, neutral

*Author for correspondence; e-mail: odl@lci.kent.edu

Liquid Crystals ISSN 0267-8292 print/ISSN 1366-5855 online © 2004 Taylor & Francis Ltd
http://www.tandf.co.uk/journals
DOI: 10.1080/02678290410001703145

particles, electrons and mixtures thereof. With respect to the treatment effect, two types of particle beam alignment method can be distinguished. In the first type, the beam is composed of particles that serve as aligning material once deposited onto a bare substrate. The deposition might be direct (thermal deposition [4], etc.) or indirect (ion beam sputtering [5], etc.). In the second type of treatment, the particle beam is used to etch an aligning layer deposited prior to irradiation. For example, Little *et al.* [6] suggested oblique irradiation of the aligning films with ion fluxes of high energy (1–3 keV). This method was further studied by Sun *et al.* [7]. Recently, the IBM group modified this procedure by using a flux of low energy ions (50–300 eV) [8–10]. The principal advantage of this innovation is that the ion beam affects only the very top layer of the aligning film. This feature helps to mitigate the generation of free radicals, which impair the performance of LC displays (LCDs). According to [8–10], the method provides excellent LC alignment on both organic and inorganic substrates.

Another example of a particle beam is the plasma flux in which the charge of the ions is compensated by electrons. Sprokel and Gibson [11] proposed to expose the bounding substrates to a 'cold' r.f. plasma carried to the substrates by a directed gas stream; reaction between plasma and substrate led to structures capable of alignment. The plasma treatment through directed gas streams can be used in both etching and deposition regimes. It has been demonstrated that both regimes are capable of producing strong planar alignment.

In the present work, we describe a different plasma alignment technique in which the aligning substrate is treated with a flux of plasma that is extracted and accelerated electrostatically. This plasma flux is generated from a reliable and simple d.c. plasma source known as the anode layer thruster (ALT). The discharge channel in the ALT used has the shape of a race track; the straight portions of this channel are used to produce sheet-like fluxes. The ALT has been designed to generate collimated particle fluxes from practically any gaseous feed. Under certain operating parameters, with an inert gaseous feed, the proposed source yields etching conditions similar to those described previously in [8–10]. An important difference, however, is that our technique produces *two* modes of planar LC alignment rather than the one described in [8–10]. The two modes are both close to the planar alignment and represent (1) tilted planar (with a small pretilt $\theta \leqslant 10^{\circ}$) and (2) strictly planar (zero tilt, $\theta = 0$) alignments, with different geometrical (easy axis direction) and energetic (strength of anchoring) properties.

2. Experimental

2.1. *Ion source and irradiation procedure*

The ALT belongs to a family of closed drift thrusters (CDTs) [12]. The CDT is an electrodynamic thruster of high thrust efficiency. In comparison with electrostatic ion thrusters, closed drift thrusters have a simpler construction. They do not require filaments or secondary electron sources to initiate the discharge current or to neutralize the beam. Since the ions are accelerated electrodynamically, no grids to extract and accelerate ions are needed. Various types of CDT are used on space satellites as ion rocket engines and in a variety of plasma etching and plasma deposition systems [12].

An ALT scheme is shown in figure 1. The source has permanent magnets at the inner and outer cathodes. The anode is mounted in the space between the inner and outer cathodes. Together these electrodes define the size and shape of the discharge channel. The ion flux is formed in crossed electric (**E**) and magnetic (**H**) fields immediately within the discharge channel. It is part of

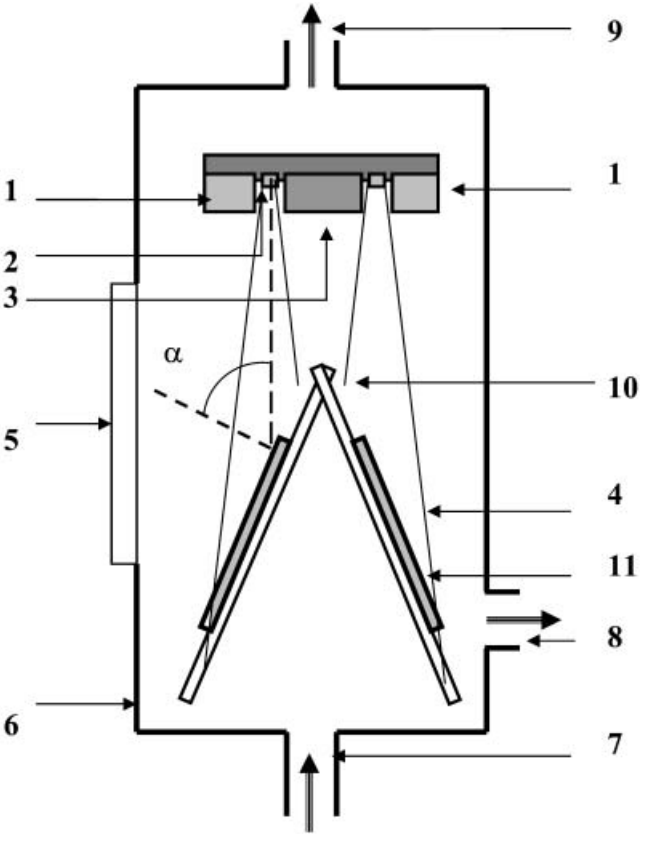

Figure 1. Scheme of anode layer thruster and irradiation method. 1 = outher cathode and N pole; 2 = anode; 3 = inner cathode and S pole; 4 = plasma flux; 5 = window; 6 = body of vacuum chamber; 7, 8, and 9 = gas valves; 10 = substrate holder; 11 = substrate.

the d.c. plasma generated in the discharge area. For more details, see refs. [12, 13].

The generated plasma flux has the shape of a hollow cylinder with a cross-section determined by the shape of the discharge channel. It may be circular or, as in the ALT used here have a race track shape. The straight portions of the race track profile are suitable for a well controlled treatment of large area surfaces, provided the sample can be translated and tilted.

Argon was used as the working gas for the non-reactive treatment of the aligning substrates. The pressure P in the source chamber was $(2\text{–}10)\times10^{-4}$ Torr, and determined the current density j of Ar^+ ions. The ion energy was controlled by the anode potential U, which was varied within the range 200–2000 eV†. Therefore, the following three plasma irradiation parameters were independently varied: (1) irradiation time τ_{exp}; (2) current density j; (3) ion energy E.

The substrate holder was mounted in a vacuum chamber just under the discharge channel (figure 1). The approximate distance between the plasma outlet and the irradiated substrate was 6 cm; the substrates of size of $30\times20\,mm^2$ were irradiated slantwise. We used two different sample settings with respect to the plasma sheet (figure 2). The plasma beam incidence angle α was varied between 0° (normal to the substrate) and 80°; see figure 1. To create alignment patterns, we used paper or plastic masks placed on the substrates to be treated.

The beam intensity profile was characterized by scanning a probe across the beam; the distribution is of Gaussian shape (figure 3, curve 1). The half-width of the beam intensity distribution corresponds to the cone of the angle $\beta\approx6°$ with the apex in the discharge area. The beam divergence within this cone was further analysed using a Faraday cup. The pinhole aperture of the cup was oriented perpendicularly to the beam propagation direction. The ion distribution behind the aperture was estimated by measuring the current in the concentric copper wire rings mounted on the bottom of Faraday cup. This distribution is shown in figure 3, curve 2. One can see that the majority of ions ($>70\%$) travel within the cone with the half angle $\gamma\approx3°$, i.e. the particle beam is well collimated. However, some ions have a path that diverges to rather large angles ($>10°$).

†More precisely, the anode potential U determines the maximum energy of the Ar^+ ions. The energy spectrum of generated ions is broad with the maximum at approximately $\frac{2}{3}eU$. In the following we consider maximum ion energy, i.e. $E=eU$.

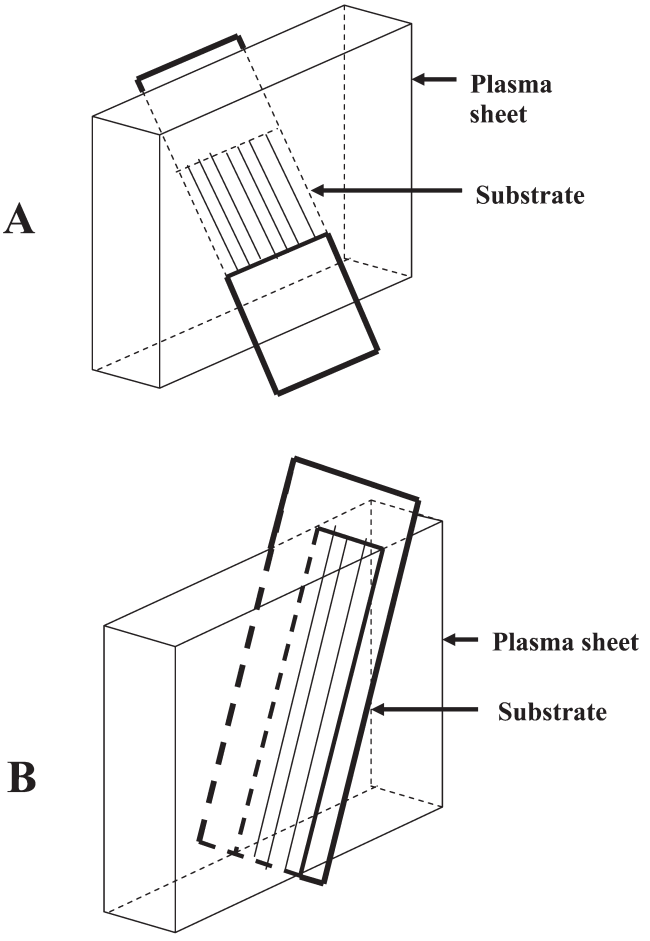

Figure 2. Two different types of sample orientation with respect to the plasma beam.

2.2. *Samples and methods of the LC alignment characterization*

We used a variety of organic polymers and inorganic coatings as aligning substrates for LC cells. Among them were polyimide PI 2555 purchased from Dupont, and polyvinylcinnamate (PVCN) and polymethylmethacrylate (PMMA) from Aldrich. The polymers were dissolved in an appropriate solvent and spin coated on the glass plates over ITO electrodes; the substrates were then baked to remove solvent. As inorganic substrates, we mainly used bare glass slides (microscope slides purchased from Fisher Scientific) and ITO coated glass slides. We also used a-C:H films obtained by plasma enhanced chemical vapour deposition [14]. The irradiation conditions were optimized for each type of substrate.

The LC alignment was studied by preparing two types of LC cell: (1) asymmetric cells in which one substrate was treated with the plasma beam, while the second substrate had a rubbed polyimide layer; (2) symmetric cells, in which both bounding plates

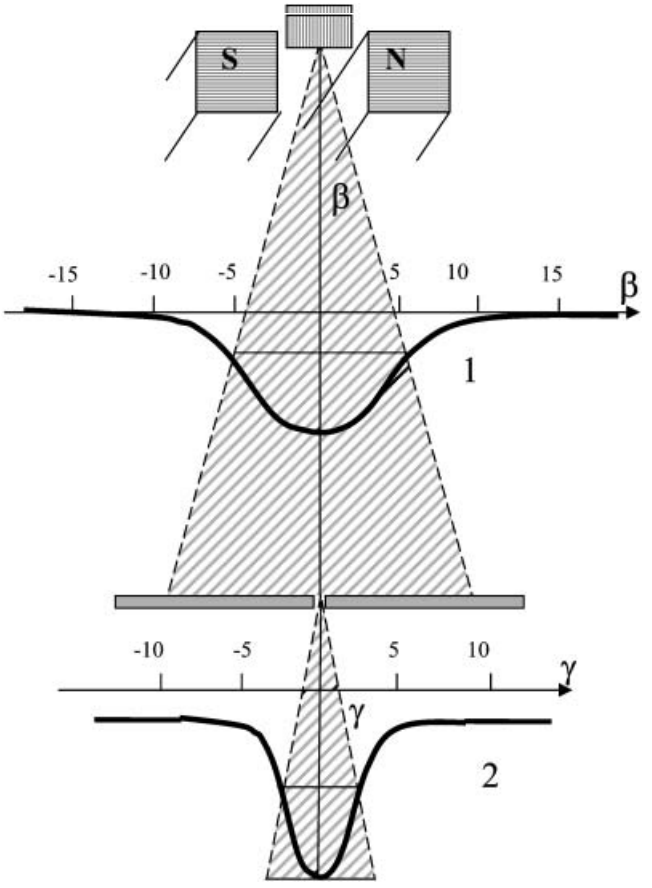

Figure 3. Scheme illustrating the beam profile (curve 1) and the beam divergence (curve 2).

were irradiated with the plasma beam. To obtain a uniform director orientation, the cells were assembled in an antiparallel fashion, so that the plasma beam treatment directions of the two opposing bounding plates were antiparallel to each other. The cell gap was kept by spacers of diameter 6 and 15 μm. The cells were filled with the nematic LCs pentylcyanobiphenyl (5CB) and ZLI4801-000 purchased from Merck.

The symmetric cells were used to measure the pretilt angle by the crystal rotation method [15]. The asymmetric cells were prepared to determine the direction of LC alignment in the plane of the plasma-treated substrate. Cells with twisted director were used to estimate the azimuthal anchoring coefficient as described previously [16,17]. The azimuthal anchoring was also characterized by the method suggested in [18]; in addition to the anchoring coefficient, this method allowed us to elucidate the conditions of easy axis gliding and LC alignment memory. Polar anchoring was characterized by the 'retardation vs. voltage' method [19].

3. Results and discussion

3.1. *LC alignment*

Uniform alignment in the LC cells with plasma-treated substrates is achieved for a wide range of irradiation parameters: $j = 0.5$–$30\,\mu A\,cm^{-2}$, $E = 200$–$2000\,eV$, $\tau_{exp} = 0.1$–$20\,min$. These ranges overlap with those used by the IBM group [8–10]; however, in contrast to their data, we observe two different modes of LC alignment, see figure 4.

In mode 1, the easy LC axis is in the incident plane formed by the direction of the beam and the normal to substrate, and tilts in the direction of the beam; the pretilt angle θ is generally non-zero. In mode 2, the easy axis is perpendicular to the plane of incidence, $\theta = 0$. Figure 5 shows that the transition from mode 1 to mode 2 is caused by the increase of current density of the argon ions. Mode 2 appears initially in the area irradiated with the central, most intensive part of the beam, see figure 5. A similar alignment transition occurs when the irradiation time increases, see figure 6. In

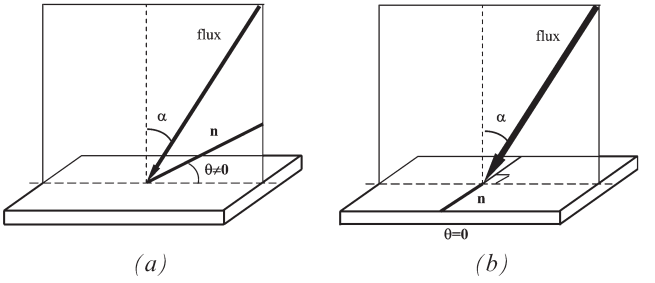

Figure 4. Irradiation geometry and LC alignment in the first (*a*) and second (*b*) modes.

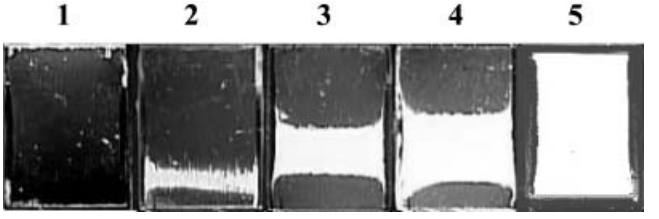

Figure 5. Photographs of a set of asymmetric cells viewed between crossed polarizers. One plate of the cells contains a rubbed PI layer, the other contains a PVCN layer treated with plasma beam in geometry A, figure 2. The plasma irradiation parameters are $\alpha = 60°$, $E = 600\,eV$, $\tau_{exp} = 10\,min$; the ion current density j is 1, 2, 5, 7, and $9\,\mu A\,cm^{-2}$ for cells 1, 2, 3, 4 and 5, respectively. The cells are 15 μm thick and filled with 5CB. The figure shows the alignment mode 1 in cell 1, regions with the 1st and 2nd alignment modes (dark and bright areas, respectively) in cells 2, 3, and 4, and alignment mode 2 in cell 5. The transition from dark to bright texture is caused by a 90° reorientation of the LC at the plasma-treated substrate. Cell area approximately $2 \times 3\,cm$.

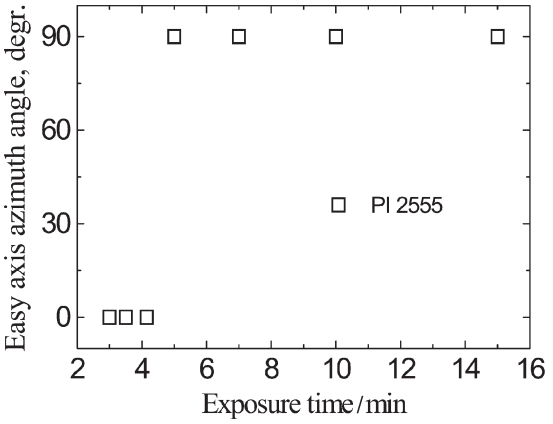

Figure 6. Azimuthal angle of the LC easy axis at the plasma-treated PI substrate as a function of irradiation time. The data are very similar for 5CB and ZLI 4801-000 nematic LCs.

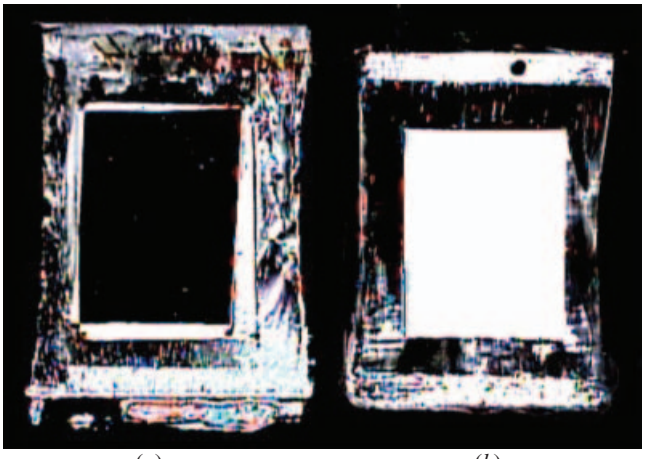

(*a*) (*b*)

Figure 7. Photographs of two asymmetric cells filled with 5CB viewed between crossed polarizers. The cells contain a rubbed PI substrate as reference and a plasma-treated glass slide as the object substrate. The object substrates were irradiated through the mask with a rectangular opening area in the middle of the substrate. The irradiation geometry and the cell assembling process were the same for both cells. The irradiation dose corresponds to mode 1 in cell (*a*), and to mode 2 in cell (*b*).The dark state of the oriented part of cell (*a*) implies that LC alignment on the plasma-treated substrate is parallel to the alignment on the reference substrate. Analogously, the bright state of cell (*b*) shows that LC alignment on the plasma-treated substrate is perpendicular to the alignment on the reference substrate. Both cells demonstrate a high quality of LC alignment.

other words, the alignment type is controlled by the irradiation dose. A change of ion energy does not cause the transition from mode 1 to mode 2. Two-mode alignment is observed for both sample settings shown in figure 2 and for both nematic materials used in the experiments.

Note that both these materials have a positive dielectric anisotropy, $\Delta\varepsilon > 0$; the same two-mode alignment has been observed for other LCs with $\Delta\varepsilon > 0$. However, our preliminary data for materials with $\Delta\varepsilon < 0$, such as the mixture MJ961180 (Merck Korea), reveal only mode 1 alignment with a high pretilt angle ($\theta > 20^\circ$). The trend is similar to the behaviour of the $\Delta\varepsilon > 0$ and $\Delta\varepsilon < 0$ LCs aligned by oblique deposition of SiO_x coatings [20,21]. In the following, we refer to materials with $\Delta\varepsilon > 0$ only; the differences in the alignment for $\Delta\varepsilon > 0$ and $\Delta\varepsilon < 0$ LCs will be discussed elsewhere.

3.1.1. *Alignment mode 1*

A typical sample aligned in mode 1 is shown in figure 7 (*a*). The pretilt angle is not zero and the LC easy axis is in the plane of incidence. The pretilt angle can be controlled in a relatively broad range $0^\circ < \theta < 10^\circ$ by changing the irradiation parameters; figure 8 shows how θ changes with the beam incidence angle α. The functions $\theta(\alpha)$ measured for different aligning films are non-monotonous with the maximum at $\alpha = 40^\circ$–50°. The variation of θ with exposure time τ_{exp} is presented in figure 9. This curve is also non-monotonous with a quasi-linear growth at small τ_{exp}, saturation and rapid decrease in the vicinity of the transition to mode 2. The pretilt angle monotonously decreases with the ion energy (anode potential), figure 10, which suggests that for an ion energy corresponding to a voltage of less than 300 V, one might achieve a pretilt angle larger than 10°. However, we could not verify this possibility as the operating voltage threshold of our source was about 300 V.

The azimuthal anchoring energy coefficient W_a in mode 1 alignment has been estimated to be of the order $10^{-6}\,J\,m^{-2}$; this is comparable to values reported for the surface memory effect [22] and photo-alignment [23]. Thus mode 1 alignment is close to the alignment mode reported by the IBM group [8–10] with the exception that the azimuthal anchoring coefficient W_a in our case is relatively low. Some other aspects of mode 1 LC alignment, including the combination of plasma treatment with phototreatment and rubbing, can be found in refs. [24, 25].

3.1.2. *Alignment mode 2*

A LC cell aligned in mode 2 is shown in figure 7 (*b*). The easy axis is perpendicular to the plane of incidence. The pretilt angle is zero, $\theta = 0$. The azimuthal anchoring corresponding to mode 2 is strong, $W_a \geqslant 5 \times 10^{-4}\,J\,m^{-2}$

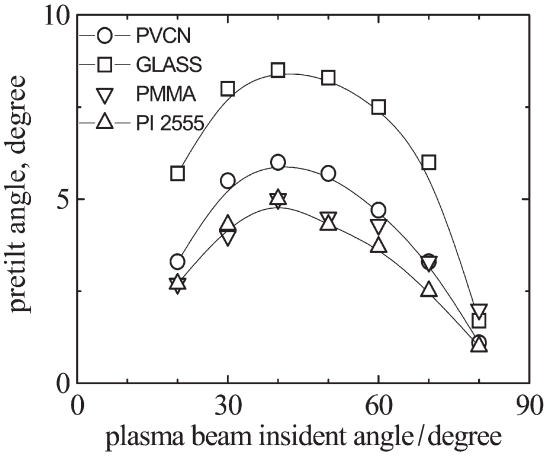

Figure 8. The pretilt angle θ vs. the plasma beam incidence angle α for different substrates in 5CB cells. The irradiation parameters for polymer and glass substrates are $j=8\,\mu A\,cm^{-2}$, $E=600\,eV$, $\tau_{exp}=1.5\,min$; and $j=2\,\mu A\,cm^{-2}$, $E=500\,eV$, $\tau_{exp}=1.5\,min$, respectively. The cell gap in each case is 15 μm.

(which is the limit of our measuring methods). No gliding of the easy axis is observed. The polar anchoring coefficient is of the order $10^{-4}\,J\,m^{-2}$. The results are similar for the polymer aligning films (PI, PVCN, PMMA) and for bare glass and are comparable to those usually reported for rubbed polymer aligning substrates. The LC alignment of mode 2 type has been previously described for some rubbing [26] and photoaligning processes [27]. Two-mode alignment was also observed for obliquely deposited SiO_x films [20,21,28], but not for etching techniques.

Note that many applications require simultaneously

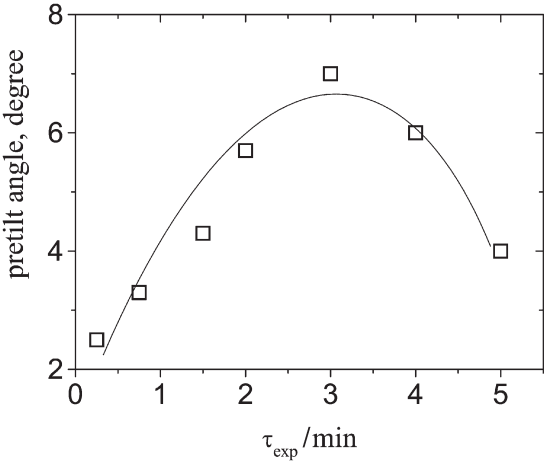

Figure 9. The pretilt angle vs. irradiation time dependence as measured for substrate PI2555 in the 5CB cell. The irradiation parameters are $\alpha=50^\circ$, $j=8\,\mu A\,cm^{-2}$, $E=600\,eV$. The cell gap is 15 μm.

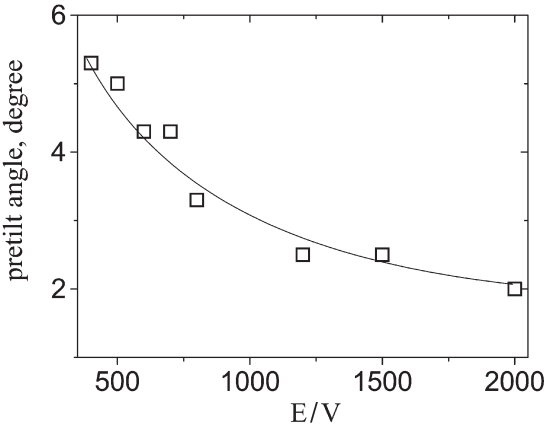

Figure 10. Pretilt angle vs. ion energy dependence obtained for a PI2555 substrate in the 5CB cell. The irradiation parameters are $\alpha=50^\circ$, $j=8\,\mu A\,cm^{-2}$, $\tau_{exp}=1.5\,min$. The cells gap is 15 μm.

a non-zero pretilt angle and a strong in-plane anchoring. ALT-generated plasma alignment can satisfy both these conditions, if one uses a procedure of subsequent steps of sample irradiation. For example, one can first align the substrate in mode 2, then reorient the substrate by 90° and plasma-align it again according to mode 1 to cause a non-zero pretilt angle θ. As we verified experimentally, the resulting alignment is characterized by both strong anchoring ($W_a \geqslant 10^{-4}\,J\,m^{-2}$) and a non-zero pretilt angle ($0^\circ < \theta < 5^\circ$).

3.1.3. *Alignment stability*

In order to check the thermal stability of LC alignment at the plasma-treated substrates, the cells were exposed to prolonged heating at 90°C over 3 h. The heating treatment caused no substantial change of alignment quality for either alignment mode. The induced alignment is also photo-resistant; we observed no deterioration of LC alignment after irradiation of our cells with unpolarized UV light ($15\,mW\,cm^{-2}$, 1 h).

The LC alignment quality does not degrade with sample aging under room conditions. At the same time, such aging may cause the decrease of pretilt angle. The characteristic time of this process is several weeks (figure 11). Pretilt angle aging can be explained by the appearance of low-molecular mass products of plasma etching at the substrate and their partial dissolution in the LC. As figure 11 illustrates, aging effects in some materials are less dramatic than in others. Therefore, one can mitigate the negative impact of aging by a proper material selection.

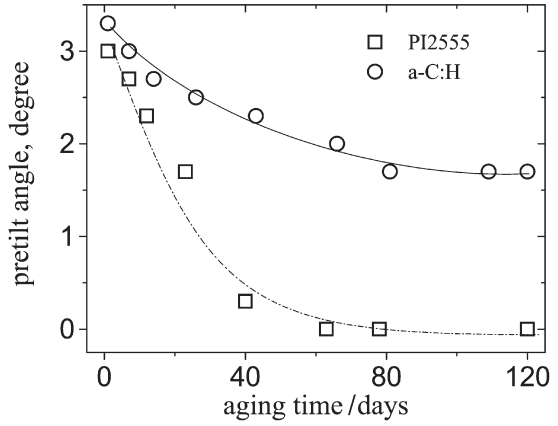

Figure 11. Pretilt angle vs. cell aging time for 5CB cells with PI2555 and a-C:H substrates. Room conditions.

3.2. *LC alignment mechanisms*

The nature of LC alignment depends on a number of factors. One of the most important is the direct anisotropic interaction between the molecules of two adjacent media. Another factor is topographical and relates to the intrinsic elasticity of the LC: if the LC is in contact with a non-flat substrate or in a non-flat sample, it will align along the direction (or directions) that yield the smallest energy of elastic distortions.

Using near-edge X-ray absorption fine structure (NEXAFS) spectroscopy sensitive to surface layers, Stöhr *et al.* [10] detected anisotropic distribution of the molecular groups at the surface of aligning films treated with an oblique ion beam. This anisotropy was explained by postulating selective destruction of molecular bonds by the ions. Qualitatively, a molecular group that extends in the direction of the incident oblique beam is less likely to be destroyed than a molecular group that extends in the direction perpendicular to the beam.

Certainly, the mechanism of angularly-sensitive destruction of molecular bonds outlined above might play an important role in the aligning mechanism of the present technique. However, the topography of the substrates can also be important, as discussed below.

We studied the surface profile of the plasma-treated substrates by atomic force microscopy (AFM, Nanoscope IIIa), figure 12. The plasma-treated surfaces become rougher than untreated substrates (A, A′), as seen in other studies [29]. In our case, plasma treatment (in both modes) creates surface features of an average size 10–100 nm, elongated along some preferred directions. In mode 1, these features seem to be randomly distributed; they are elongated along the plane of incidence (figure 12, B and B′). In mode 2 a rough uneven ridge system develops and extends perpendicularly to the plane of incidence (figure 12, C and C′). As the system of ridges does not break the symmetry with respect to the plane of incidence, no pretilt should be generated in mode 2, as observed.

As demonstrated long ago by Berreman, for a substrate that favours in-plane orientation the 'groves' and 'ridge' topography determines both the direction (usually along the grooves) and the strength of in-plane anchoring [30]. According to the Berreman model for a sinusoidally modulated substrate, the azimuthal anchoring coefficient W_a is determined by the amplitude a and the wavelength Λ of the surface modulations, $W_a = \frac{1}{2}Ka^2\left(\frac{2\pi}{\Lambda}\right)^3$. With the typical $a = 0.4$–1 nm and $\Lambda = 10$–50 nm and the Frank elastic constant $K = 10$ pN, one arrives at $W_a \approx (10^{-6}$–$10^{-4})\,\mathrm{J\,m^{-2}}$ which is within the range of experimental data. Therefore, surface topography might be as important as the selective chemical bond scission, similar to the case of oblique deposition of SiO_x [4, 28]. Significant modification of the surface profile in the present case of plasma etching and in SiO_x deposition might explain why the azimuthal anchoring is stronger than in the case of photoalignment, which usually produces smooth surface profiles [31, 32].

It is important to clarify which of the plasma components (UV light, electrons, ions, neutral atoms) plays the most significant role in LC alignment. To elucidate the role of UV light, the photosensitive PVCN film was irradiated with a plasma beam through a quartz plate transparent for deep UV irradiation. The UV/Vis spectrum of the film exhibited changes confirming UV light action; however, this UV irradiation did not result in LC alignment. This, as well as the fact of LC alignment at the plasma-treated non-photosensitive substrates (glass and ITO), shows that the UV component may play only a secondary role in LC plasma-induced alignment. To test a hypothesis that the LC alignment might be caused by the electron component in the ALT flux, we used an indirect experiment, by treating the substrates with a sheet-like e-beam generated by the electron beam machine CB150 from Energy Sciences Inc. (USA). The operating voltage and current density were 175 keV and $180\,\mu\mathrm{A\,cm^{-2}}$, respectively. During irradiation the samples were positioned obliquely to the e-beam ($30^\circ < \alpha < 70^\circ$) and moved with a velocity of $0.19\,\mathrm{m\,s^{-1}}$. These conditions correspond to an irradiation dose of about 100 kGy. The e-beam-treated substrates show no aligning capabilities when used in LC cells. These results, although very preliminary, indicate that the main mechanism of alignment by ALT-generated plasma fluxes involves primarily ions and, perhaps, neutral atoms that might also be present (in much smaller quantities) in the plasma flux.

Let us now discuss the possible mechanisms of the

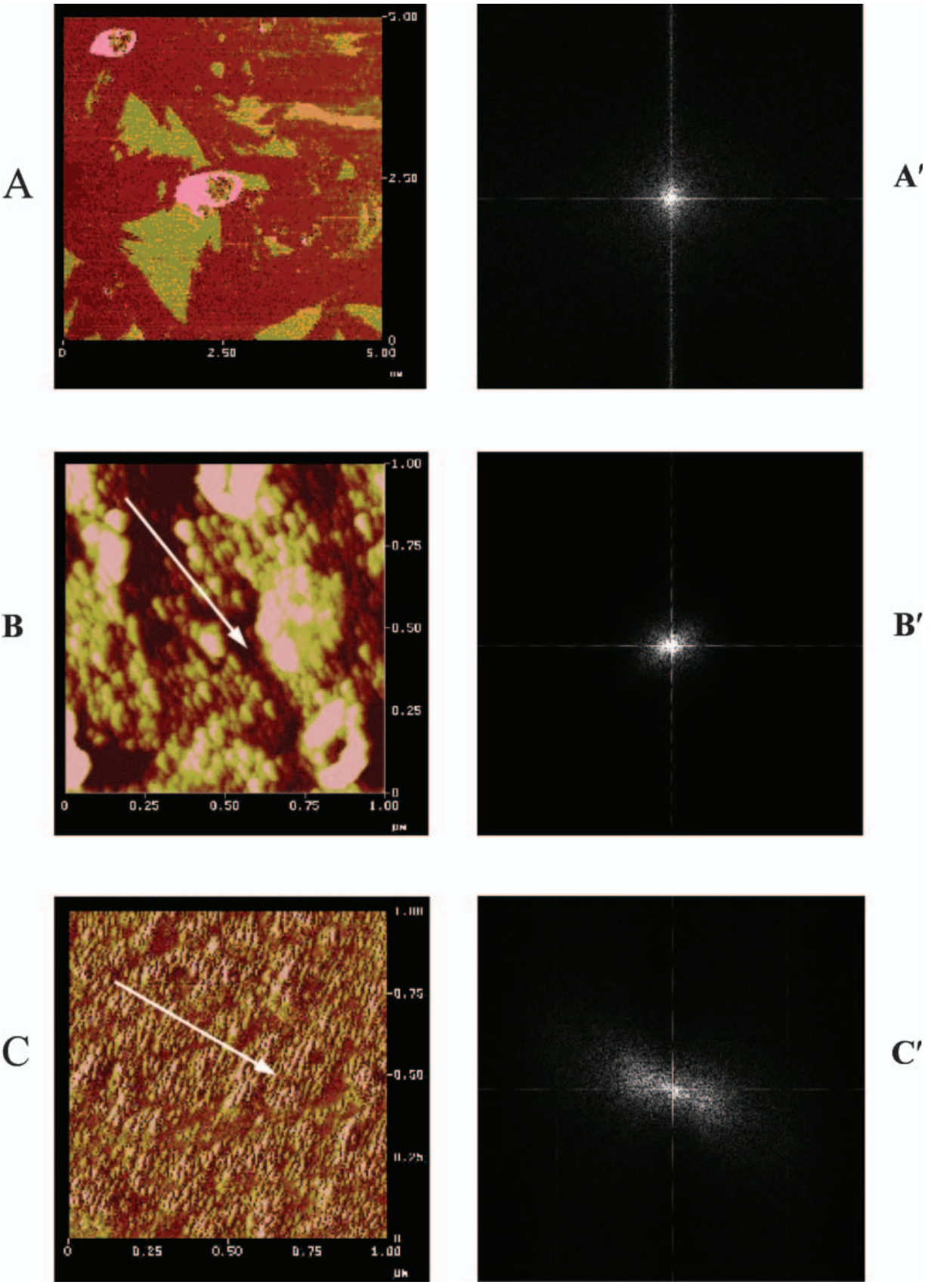
A
A′
B
B′
C
C′
5.00
2.50
0
2.50
5.00
1.00
0.75
0.50
0.25
0
0.25
0.50
0.75
1.00

two-mode alignment. As mentioned above, similar multi-mode alignment regimes have already been described for alignment by rubbed polymer films [26], photoalignment [27] and SiO_x deposition [28]. In the most popular rubbing technique, the director usually aligns along the direction of rubbing. However, a perpendicular mode of alignment, similar to the aligning mode 2 described above, is also known, as reviewed in a great detail recently [26]. Lee *et al.* [26] demonstrated that, at least in the case of rubbed polysterene films, rubbing might cause 'grooves' perpendicular to the rubbing direction. Physically, such topography is natural, as many elastic bodies and films develop wrinkles perpendicular to the shear direction (the simplest experiment can be performed by rubbing a skin with a finger).

In the photoalignment technique, in which the topography changes little, the easy axis is determined by the orientational distribution of photosensitive fragment and their photoproducts. If there are different types of fragment with different aligning tendencies, one might observe several alignment modes [27].

In SiO_x deposition [4, 5, 28], relatively small deposition angles ($40^\circ < \alpha < 70^\circ$) cause the easy axis to be perpendicular to the plane of the incidence of the particle beam. For grazing deposition ($\alpha \geqslant 80^\circ$), the easy axis is in the plane of incidence with a tilt toward the evaporation direction. This alignment transition is explained by the experimentally detected change in the anisotropy direction of the surface profile. Tilted deposition results in the formation of elongated elevations (needles, columns) tilted in the plane of deposition. Their growth results in the merging of individual needles into rows and also in a 'self-shadowing' effect, considered by Smith *et al.* [33]. The deposited grains prevent the new particles from reaching the substrate in the shadow of the grain; consequently, vacant regions are left in the film and individual grains of material eventually join a two-dimensional ridge structure, with the long axis perpendicular to the plane of incidence. The study of surface topography suggests that the growing needles indeed form rows elongated predominantly perpendicularly to the plane of incidence. Depending on the ratio of the width of the needle (and row) to the average repeat distance between the rows along the direction of deposition, the orientation might be of either first or second type. Usually, with $40^\circ < \alpha < 70^\circ$ the alignment is perpendicular to the deposition plane; the reason is that the repeat distance is relatively small and director orientations other than perpendicular to the plane of incidence would lead to strong elastic distortions. In contrast, with grazing deposition, the rows of needles are far apart and the LC can be aligned parallel to the plane of incidence.

The topographic features observed in the plasma etching technique are somewhat similar to those detected for films obtained by deposition. The different modes of alignment might be caused by an effect similar to the self-shadowing effect above, as the etched portions of the substrate, with the slope along the direction of beam, are less exposed to the flux.

Apart from this 'shadow' effect, the topography changes observed in the AFM studies and manifested in the transformation of mode 1 into mode 2, might also be related to other mechanisms, in particular, to the finite divergence of the ALT plasma beam. Mode 2 might be provoked by ions that deviate from the average direction of deposition. Indirect evidence for this possibility comes from a rather surprising fact that mode 2 alignment was never described for substrates treated obliquely with ion beams generated by the Kaufman plasma source [8–10, 34–37]. The irradiation parameters in the cited experiments were probably in the region of values where the topography does not change enough to cause mode 2. Clearly, further studies are needed to elucidate the mechanisms in detail.

3.3. *Practical value*

It is of interest to compare the technique to other plasma methods that include deposition of various films [38–40] and post-deposition treatments, mainly by bombardment with reactive ions [41–43]. All these methods are capable of producing various values of the zenithal anchoring coefficient and pretilt angle but not a uniform planar alignment; mostly because the substrates are placed in the gas discharge area where the plasma treatment is practically isotropic. Sprokel and Gibson [11] proposed a *directed* plasma flux and anisotropic treatment, which resulted in a uniform planar alignment. This was achieved by the use of a modified r.f. plasma etcher in which reactive plasma was extracted and carried onto substrates by the gas stream. In our experiments, plasma is extracted and accelerated electrostatically to relatively low energies, and treats only a thin layer of the substrate, similar to the procedure described for ion beams [8–10]. Thus the ALT source allows one to combine the advantageous

Figure 12. AFM images of the untreated (A) and plasma-treated glass substrates (B, C). The substrates B and C were treated for alignment modes 1 and 2, respectively; the arrow shows the direction of the plasma beam. Frames A′, B′ and C′ are Fourier transformations of the images A, B and C.

anisotropic treatment with collimated plasma fluxes and the optimized energies of ions. Note that the ALT source can be scaled up to treat substrates of large size (meters). Reliability, simplicity of construction, high thrust efficiency and ease of treatment of substrates make this source attractive for technological applications.

One of the main advantages of the described procedure is that it yields several regimes of LC alignment, namely:

(1) Mode 1. Planar alignment with a weak azimuthal anchoring ($W_a = 10^{-6}$–$10^{-5}\,J\,m^{-2}$) and relatively high pretilt angle $\theta = (5^\circ$–$10^\circ)$.
(2) Mode 2. Planar alignment with strong anchoring ($W_a > 10^{-4}\,J\,m^{-2}$) and zero pretilt angle.
(3) Subsequent treatment using combinations of the basic two modes above; planar alignment with strong anchoring ($W_a > 10^{-4}\,J\,m^{-2}$) and moderate pretilt angle $\theta = (0^\circ$–$5^\circ)$.

Each of these regimes is attractive for modern LCD technologies. The first alignment regime may be useful for LCDs based on easy axis gliding [44]. The second regime is promising for bistable nematic displays [45]. The third regime may replace the standard rubbing procedure widely used in modern LCD technology.

This two-mode alignment opens new opportunities for the patterning of LC alignment. For example, two-domain azimuthal patterning can be realized with only one masking step, with no rotation of the substrate. The processing scheme and photographs of a sample aligned in this manner are presented in figure 13. Evidently, all the patterning procedures described for other etching alignment methods are feasible for our case, too. Moreover, for sample patterning, the plasma alignment method may be combined with other methods of LC alignment.

The electro-optic properties of cells aligned by plasma treatment are very similar to those of cells prepared with the rubbing method [25]. We observed no substantial differences in dielectric constants ε' and ε'', and in their frequency dependences, for LC cells prepared by these two methods.

Finally, it is worth mentioning that the proposed aligning procedure is compatible with other vacuum processes employed in LCD industry (ITO deposition, TFT coating, vacuum filling of LCD, etc.). One might expect that an entirely vacuum technological line for LCD production could strongly reduce the well known problems related to dust, humidity, air ions, etc.

4. Conclusions

We have presented a new ion/plasma aligning technique that yields two basic modes of uniform LC alignment on a variety of organic and inorganic

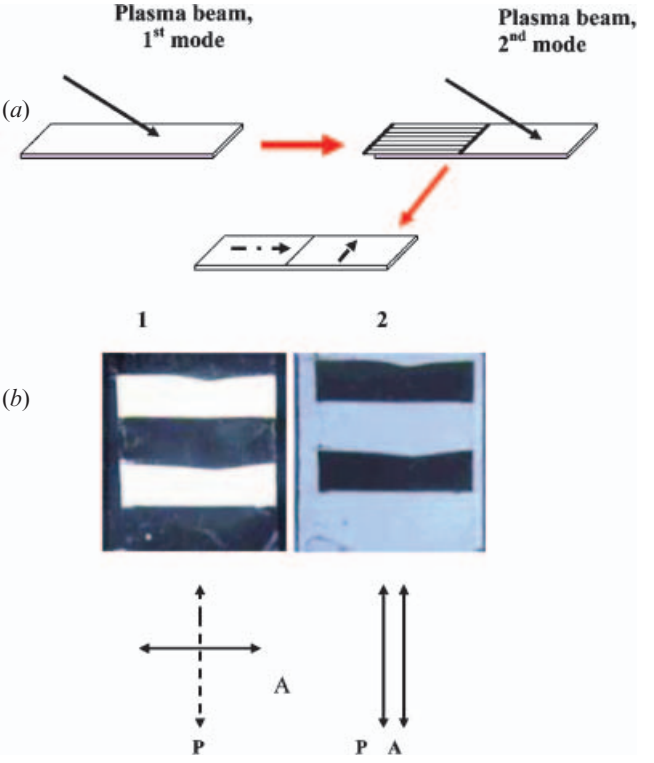

Figure 13. (*a*) The patterning scheme based on alignment transition mode 1 to mode 2; (*b*) photographs of a LC cell viewed between a pair of crossed and parallel polarizers. The cell is asymmetric with one rubbed PI substrate and one plasma-treated PI substrate. To obtain the pattern, the whole area of the latter substrate was first irradiated with the plasma beam ($E = 600\,V$, $j = 8\,\mu A\,cm^{-2}$, $\alpha = 60^\circ$) for $\tau_{exp} = 2.5\,min$; the portions of the substrate were then covered with the mask and the remaining regions exposed to the same plasma beam for an additional $\tau_{exp} = 10\,min$. The dark and bright areas of the texture correspond to two different LC orientations at the plasma-treated substrate: parallel and perpendicular to the alignment direction on the PI substrate, respectively.

substrates: (1) tilted with the director in the plane of incidence and (2) planar with the director perpendicular to the plane of incidence and thus zero pretilt. The plasma treatment results in anisotropic modification of the aligning substrates; the different modes of alignment are related to different topographical features of the treated substrates. In particular, in mode 2, one observes series of ridges developing at the treated substrate in a direction perpendicular to the plane of incidence.

The alignment in both modes is of high quality with a good thermal and photostability. The technique allows one to control the pretilt angle and to obtain a high in-plane (azimuthal) anchoring coefficient. The

two-mode alignment opens new opportunities for patterning of the aligning substrates.

We thank I. Dozov and P. Martinot-Lagarde (Nemoptic, France), L.-C. Chien (Liquid Crystal Institute, USA) for fruitful discussions. We also gratefully acknowledge the support of I. Dozov in anchoring studies and U. Maschke (University of Lille, France) in e-beam irradiations.

References

[1] Dyadyusha, A., Kozenkov, V., Marusii, T., Reznikov, Yu., Reshetnyak, V., and Khizhnyak, A, 1991, *Ukr. Phys. J.*, **36,** 1059.
[2] Schadt, M., Schmidt, K., Kozinkov, V., and Chigrinov, V., 1992, *Jpn. J. appl. Phys.*, **31,** Part 1, 2155.
[3] Hasegawa, M., 2000, *Jpn. J. appl. Phys.*, **39,** Part 1, 1272.
[4] Janning, J., 1972, *Appl. Phys. Lett.*, **21,** 173.
[5] Motohiro, T., and Taga, Y., 1990, *Thin solid Films*, **185,** 137.
[6] Little, M. J., Garvin, H. L., and Lee, Y.-S., 1979, US Patent No 4 153 529.
[7] Sun, Z. M., Engels, J. M., Dozov, I., and Durand, G., 1994, *J. Phys. II Fr.*, **4,** 59.
[8] Chaudhari, P., Lacey, J., Lien, S. A., and Speidell, J., 1998, *Jpn. J. appl. Phys.*, **37,** L55.
[9] Chaudhari, P., Lacey, J., Doyle, J., Galligan, E., Lien, S. C. A., Callegari, A., Hougham, G., Lang, N. D., Andry, P. S., John, R., Yang, K. H., Lu, M. H., Cai, C., Speidell, J., Purushothaman, S., Ritsko, J., Samant, M., Stohr, J., Nakagawa, Y., Katoh, Y., Saitoh, Y., Sakai, K., Satoh, H., Odahara, S., Nakano, H., Nakagaki, J., and Shiota, Y., 2001, *Nature*, **411,** 56.
[10] Stöhr, J., Samant, M. G., Lüning, J., Callegari, A. C., Chaudhari, P., Doyle, J. P., Lasey, J. A., Lien, S. A., Purushothanam, S., and Speidell, J. L., 2001, *Science*, **292,** 2299.
[11] Sprokel, G. J., and Gibson, R. M., 1977, *J. electrochem. Soc.*, **124,** 559.
[12] Zhurin, V., Kaufman, H., and Robinson, R., 1999, *Plasma Sources Sci. Technol.*, **8,** 1.
[13] Keem, J. E., 2001, in Proceedings of the 44th Annual Technical Conference of SVC, 1.
[14] Yaroshchuk, O., Kravchuk, R., Dobrovolskyy, A., Klyui, N., and Korneta, O., 2002, in Proceedings of the XIth International Symposium. *Advanced Display Technologies*, 8–12 September, 2002, Crimea, Ukraine.
[15] Baur, G., Wittwer, V., and Berreman, D. W., 1976, *Phys. Lett., A*, **56,** 142.
[16] Rapini, A., and Papoular, M., 1969, *J. Phys. Colloq. (Fr.)*, **30,** C4-54.
[17] Bryan-Brown, G., and Sage, I., 1996, *Liq. Cryst.*, **20,** 825.
[18] Polossat, E., and Dozov, I., 1996, *Mol. Cryst. liq. Cryst*, **282,** 223.
[19] Nastishin, Yu. A., Polak, R., Shiyanovskii, S. V., Bodnar, V., and Lavrentovich, O. D., 1999, *J. appl. Phys.*, **86,** 4199.
[20] Lu, M., Yang, K. H., and Chey, J. S., 1999, *IDW'99*, 121.
[21] Lu, M., Yang, K. H., Nakasogi, T., and Chey, J. S., 2000, *SID 00 Dig.*, 446.
[22] Barberi, R., Dozov, I., Giocondo, M., Iovane, M., Martinot-Lagarde, Ph., Stoenescu, D., Topchev, S., and Tsonev, L., 1998, *Eur. Phys. J.*, **B6,** 83.
[23] O'Neill, M., and Kelly, S. M., 2000, *J. Phys. D: appl. Phys.*, **33,** R67.
[24] Yaroshchuk, O., Zakrevskyy, Yu., Dobrovolskyy, A., and Pavlov, S., 2001, *Proc. SPIE*, **4418,** 49.
[25] Yaroshchuk, O., Kravchuk, R., Dobrovolskyy, A., and Pavlov, S., 2002, *Proc. Eurodisplay'02*, 421.
[26] Lee, S. W., Chae, B., Kim, H. C., Lee, B., Choi, W., Kim, S. B., Chang, T., and Ree, M., 2003, *Langmuir*, **19,** 8735.
[27] Reznikov, Yu., Yaroshchuk, O., Gerus, I., Homuth, A., Pelzl, G., Weissflog, W., Kim, K. J., Choi, Y. S., and Kwon, S. B., 1998, *Mol. mater.*, **9,** 333.
[28] Urbach, W., Boix, M., and Guyon, E., 1974, *Appl. Phys. Lett.*, **25,** 479.
[29] Greenwood, O. D., Hopkins, J., and Badyal, J. P. S., 1997, *Macromolecules*, **30,** 1091.
[30] Berreman, D.W., 1972, *Phys. Rev. Lett.*, **28,** 1683.
[31] Cull, B., Shi, Y., Kumar, S., and Schadt, M., 1996, *Phys. Rev. E*, **53,** 3777.
[32] Jackson, P. O., Bergman, G., Hogg, J. H. C., O'Neill, M., Hindmarsh, P., Kelly, S. M., and Clark, G. F., 2002, *Synth. Met.*, **127,** 95.
[33] Smith, D. O., Cohen, M. S., and Weiss, G. P., 1960, *J. appl. Phys.*, **31,** 1755.
[34] Kato, Y., Nakagawa, Y., Saitoh, Y., Satoh, H., Odahar, S., Chaudhari, P., Doyle, J., Lien, S. A., Callegari, A., Ritsko, J., Samant, M., and Stohr, J., 2002, *Eurodisplay 02*, 525.
[35] Hwang, J. Y., Jo, Y. M., Seo, D. S., Rho, S. J., Lee, D. K., and Baik, H. K., 2002, *Jpn. J. appl. Phys.*, **41,** L654.
[36] West, J., Su, L., Artyushkova, K., Farrar, J., Fulghum, J., and Reznikov, Y., 2002, *SID 02 Dig.*, 1102.
[37] Yang, K. H., Liang, G. T., Tanaka, S., and Endoh, H., 2003, *Proc. IDMC'03*, 82.
[38] Dubois, J. C., Gazard, M., and Zann, A., 1974, *Appl. Phys. Letters*, **24,** 297.
[39] Watanabe, R., Nakano, T., Satoh, T., Hatoh, H., and Ohki, Y., 1987, *Jpn. J. appl. Phys.*, **26,** 373.
[40] Vangonen, A. I., and Konshina, E. A., 1997, *Mol. Cryst. liq. Cryst.*, **304,** 507.
[41] Shahidzadeh, N., Merdas, A., and Urbach, W., 1998, *Langmuir*, **14,** 6594.
[42] Fonseca, J.G., Charue, P., and Galerne, Y., 1999, *Mol. Cryst. liq. Cryst*, **329,** 597.
[43] Kurchatkin, S. P., Muravyeva, N. A., Mamaev, A. L., Sevostyanov, V. P., and Smirnova, E. I., 1996, Russian Patent No 2 055 384.
[44] Kurioz, Yu., Reshetnyak, V., and Reznikov, Yu., 2002, *Mol. Cryst. liq. Cryst*, **375,** 535.
[45] Dozov, I., Nobili, M., and Durand, G., 1997, *Appl. Phys. Lett.*, **70,** 1179.